Photochemistry and Photobiology, 2015, 91: 92–101

Solar UV Irradiances Modulate Effects of Ocean Acidification on the Coccolithophorid *Emiliania huxleyi*

Kai Xu[1,2] and Kunshan Gao*[1]

[1]State Key Laboratory of Marine Environmental Science, Xiamen University, Xiamen, China
[2]Department of Biological Sciences, University of Southern California, Los Angeles, CA

Received 9 April 2014, accepted 12 October 2014, DOI: 10.1111/php.12363

ABSTRACT

***Emiliania huxleyi*, the most abundant coccolithophorid in the oceans, is naturally exposed to solar UV radiation (UVR, 280–400 nm) in addition to photosynthetically active radiation (PAR). We investigated the physiological responses of *E. huxleyi* to the present day and elevated CO_2 (390 *vs* 1000 μatm; with pH_{NBS} 8.20 *vs* 7.86) under indoor constant PAR and fluctuating solar radiation with or without UVR. Enrichment of CO_2 stimulated the production rate of particulate organic carbon (POC) under constant PAR, but led to unchanged POC production under incident fluctuating solar radiation. The production rates of particulate inorganic carbon (PIC) as well as PIC/POC ratios were reduced under the elevated CO_2, ocean acidification (OA) condition, regardless of PAR levels, and the presence of UVR. However, moderate levels of UVR increased PIC production rates and PIC/POC ratios. OA treatment interacted with UVR to influence the alga's physiological performance, leading to reduced specific growth rate in the presence of UVA (315–400 nm) and decreased quantum yield, along with enhanced nonphotochemical quenching, with addition of UVB (280–315 nm). The results clearly indicate that UV radiation needs to be invoked as a key stressor when considering the impacts of ocean acidification on *E. huxleyi*.**

INTRODUCTION

Coccolithophores perform calcification as well as photosynthesis, playing important roles in marine biogeochemical processes (1). However, such roles were supposed to be affected by changing seawater carbonate chemistry due to increasingly dissolved CO_2 from the atmosphere (2,3). *Emiliania huxleyi* is the most abundant species of coccolithophore and has been intensively examined for its responses to ocean acidification (4–6). Generally, ocean acidification (OA) is known to reduce calcification of most coccolithophores, but to stimulate or weakly influence photosynthesis and growth rates (7–10). However, enhanced calcification (per cell) of some *E. huxleyi* strains under elevated CO_2 conditions has also been observed (11–13). In most of the reported studies to date, the coccolithophore cells were grown under indoor (usually low) artificial constant light levels and little is known about their performance under naturally fluctuating solar irradiances (6).

Marine phytoplankton under natural conditions are usually exposed to many environmental changes, such as temperature, nutrient availability, solar irradiances, mixing and dissolved oxygen levels, in addition to spatio-temporal changes in seawater carbonate chemistry. The atmospheric CO_2 level will increase to 1000 ppmv and pH will drop up to 0.3–0.4 unit by the end of this century relative to the current level according to the IPCC A1F1 scenario, with the global surface temperature rising by 4°C (14). As a result of ocean warming, the thickness of the upper mixing layer (UML) will be reduced, thus phytoplankton in UML will receive more solar radiation (15,16). In addition, multifaceted effects of environmental factors, including solar radiation (280–700 nm), on marine organisms and ecosystems should be considered in order to predict OA-related effects.

Phytoplankton cells are exposed to solar radiation, including photosynthetically active radiation (PAR, 400–700 nm) as well as UV radiation (UVR, 280–400 nm). In addition, UVR at 305 nm and 340 nm could, respectively, penetrate (at 1% of surface intensity) as deep as 56 m and 118 m in open oceans (17) and fluctuates daily and seasonally. Diurnal sunlight variation could exert a significant influence on phytoplankton photophysiology and cellular energy allocation to growth (18,19), with UVR, especially UVB (280–315 nm), affecting many important metabolic processes and marine primary productivity (20,21). It has been shown that 3 h exposure of OA-treated *E. huxleyi* to PAR+UVA (315–700 nm) or PAR + UVA + B (280–700 nm) reduced calcification and photosynthetic carbon fixation relative to PAR alone (22). On the other hand, UVR inhibited the growth rate of *E. huxleyi,* with increased coccolith coverage per cell compared with PAR alone treatment (23). The coccoliths of *E. huxleyi* are known to shield off a significant amount of UVR and could play a role in photoprotection (22,23). However, little has been documented on effects of OA on morphology, physiology and molecular processes of phytoplankton when the cells are grown under fluctuating solar radiation (6). Therefore, additional knowledge is necessary to fully understand the influence of OA in natural environments.

Algal calcification is a biologically controlled process, which uses metabolic energy to decrease entropy during the formation of $CaCO_3$ crystals (24) and to maintain the calcifying system, including intracellular pH homeostasis, Ca^{2+} and HCO_3^- transporters and coccolith vesicles (25,26). Thus, coccolithophore's

*Corresponding author e-mail: ksgao@xmu.edu.cn (Kunshan Gao)

Table 1. Carbonate chemistry parameters of the outdoor experiments. Data are the means ± SD (n = 3). LC and HC represent cells that grew at ambient (390 μatm) and enriched (1000 μatm) CO_2 concentration respectively.

Treatments		pH_{NBS}	TA (μmol kg^{-1})	pCO_2 (μatm)	DIC (μmol kg^{-1})	CO_2 (μmol kg^{-1})	HCO_3^- (μmol kg^{-1})	CO_3^{2-} (μmol kg^{-1})
P	LC	8.20 ± 0.01$^+$	2454 ± 17	398 ± 8$^+$	2163 ± 17$^+$	13 ± 0.3$^+$	1943 ± 17$^+$	207 ± 2$^+$
	HC	7.86 ± 0.01$^+$	2472 ± 51	987 ± 13$^+$	2344 ± 48$^+$	32 ± 0.4$^+$	2205 ± 44$^+$	107 ± 3$^+$
PA	LC	8.20 ± 0.02$^\#$	2484 ± 30	399 ± 14$^\#$	2188 ± 18$^\#$	13 ± 0.5$^\#$	1965 ± 11$^\#$	211 ± 9$^\#$
	HC	7.86 ± 0.01$^\#$	2482 ± 18	991 ± 22$^\#$	2353 ± 14$^\#$	32 ± 0.7$^\#$	2214 ± 11$^\#$	108 ± 3$^\#$
PAB	LC	8.20 ± 0.01*	2503 ± 51	402 ± 4*	2206 ± 41*	13 ± 0.1*	1981 ± 33*	212 ± 8*
	HC	7.86 ± 0.01*	2471 ± 28	978 ± 14*	2342 ± 23*	32 ± 0.5*	2202 ± 21*	108 ± 3*

The superscripts "$^+$", "$^\#$" and "*" respectively denote significant differences between two CO_2 treatments ($P < 0.05$) under P, PA and PAB exposure.

calcification indirectly depends on the received light energy supplied by solar radiation or artificial light. On the other hand, the calcification process could act to dissipate excess light energy to protect the photosynthetic machinery when *E. huxleyi* cells are light-stressed (27,28). Coccolithophores are known to calcify less, with more malformed coccoliths, under simulated OA conditions (7,8,29). In addition to the protective roles of coccoliths for *E. huxleyi* (22), it is most likely that a reduced thickness of the cocolith layer due to progressive OA will alter its photobiological responses (28–30). Thus, the responses of *E. huxleyi* to elevated CO_2 concentrations could be modulated by changing levels of UVR and PAR in terms of its morphology, growth, photosynthesis and particulate inorganic and organic carbon production. In this study, *E. huxleyi* was incubated under different light treatments to investigate physiological effects of OA under constant indoor light regimes and natural solar irradiances.

MATERIALS AND METHODS

The calcifying strain, CS-369, of the coccolithophore *Emiliania huxleyi* used in this study was obtained from the Commonwealth Scientific and Industrial Research Organisation (CSIRO, Australia). The cells were grown in artificial seawater (except for $NaHCO_3$, which was adjusted to 2.2 mmol L^{-1}) enriched with vitamins and trace metals according to the protocol for Aquil medium (31). In addition, the nitrate and phosphate concentrations of the media were added in a ratio of 16:1, respectively 100 and 6.25 mmol L^{-1}. The photoperiod was 12:12 light:dark and growth temperature was 20°C. The media were pre-equilibrated to target CO_2 concentrations by bubbling (500 mL min^{-1}, at least 48 h) with outdoor air (390 μatm CO_2) or CO_2-enriched air (1000 μatm CO_2). The CO_2-enriched air was generated by mixing outdoor air with pure CO_2 by a solenoid valve in the plant CO_2 chamber (HP1000G-D, Wuhan Ruihua Instrument & Equipment Ltd, China). Cells were inoculated into 500 mL glass bottles or quartz tubes and closed immediately to avoid further CO_2 exchange. All of the cultures in this study were diluted every 3–4 days to maintain the final cell densities in a range of ~0.5–1.2 × 10^5 mL^{-1} and the stability of carbonate chemistry (Table 1). The pH and total alkalinity (TA) were measured using a Potentiometric Titrator (DL15, Mettler-Toledo, Schwerzenbach, Switzerland), which was calibrated with NBS buffer solutions of pH 4, 7 and 10. An open-cell titration procedure was chosen to measure TA (32). The pH was measured with every dilution and the drifts were less than 0.07 unit. TA, pH, salinity, nutrient concentrations and temperature were used to estimate all other parameters by applying the CO2sys program (33).

The *E. huxleyi* strain CS-369 had been maintained in our laboratory for about 5 years under low photosynthetically active radiation (PAR,

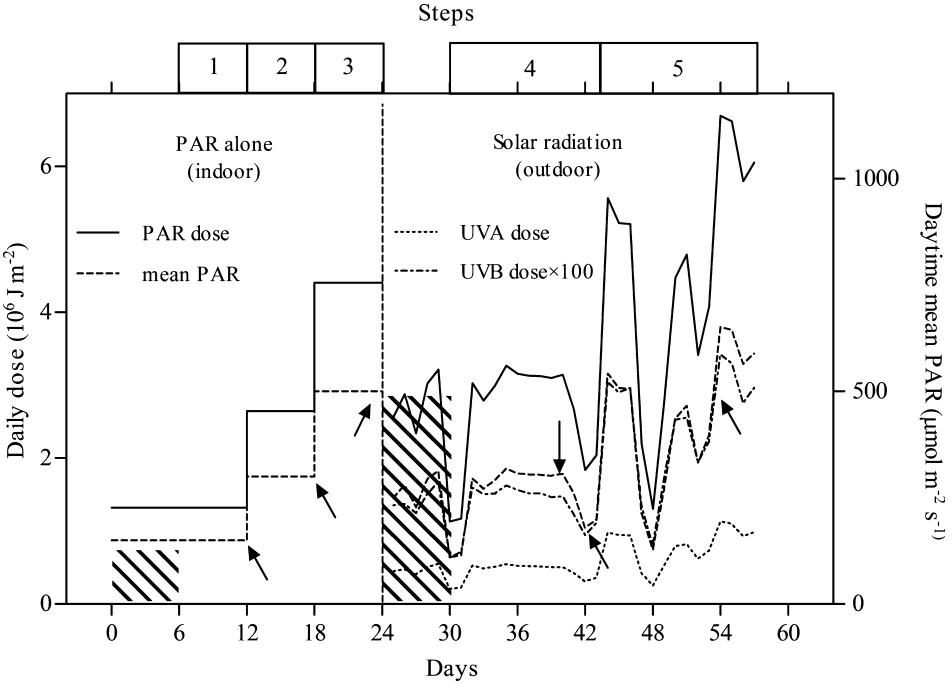

Figure 1. Daily doses of PAR, UVA, and UVB and daytime PAR (average value of light period) during the indoor (left side) and outdoor (right side separated by the broken vertical line) cultures. The cultures experienced five light treatments step by step. The shaded areas (6 days) represent the periods of pre-acclimation. Day 57 is the final day which represents 2011 July 25. The black arrows indicate the day for sample POC and PIC.

400–700 nm, about 50 μmol m^{-2} s^{-1} with 12: 12 light:dark photoperiod) without UV radiation (UVR, 280–400 nm). In this study, the cultures were acclimated step-by–step to different light treatments in order to avoid acute light shock (Fig. 1): (1) The cultures were pre-acclimated to the two CO_2 concentrations under an indoor constant PAR level of 150 μmol m^{-2} s^{-1} for 6 days, and then allowed to grow for another 6 days for the experiments; (2) Subsequently, the exposed PAR level was raised to 300 μmol m^{-2} s^{-1} and maintained for 6 days; (3) Then the PAR level was raised to 500 μmol m^{-2} s^{-1} and sustained for 6 days. (4) Following the indoor growth, the cells were transferred to outdoor incident solar radiation. They were pre-acclimated to 28% (daytime PAR average of about 270 μmol m^{-2} s^{-1}) natural solar radiation treatments (covered with two layers of neutral density screen) for 6 days, then the cultures were maintained for another 13 days for the experiments; (5) Thereafter, the level of solar radiation was increased to 56% with a daytime PAR average of about 500 μmol m^{-2} s^{-1} for 14 days by covering the quartz tubes with only one layer of neutral density screen. In brief, the cells grew at each light treatment for at least 10 generations before the data were obtained. To test the influence of UVR, three solar radiation treatments were carried out: (1) PAR alone (P), quartz tubes covered with a 395 nm cut-off foil (Ultraphan UV Opak, Digefra, Munich, Germany), transmitting irradiance above 395 nm; (2) PAR + UVA (PA), quartz bottles covered with 320 nm cut-off foil (Montagefolie, Folex, Dreieich, Germany), transmitting wavelength above 320 nm; and (3) PAR + UVA + B (PAB), quartz tubes without cover that transmit irradiances above 280 nm. The transmission spectra of these foils and quartz tubes are given elsewhere (34). All of the quartz tubes were placed in a water bath and the temperature was controlled at 20°C by a cooling system (CPT-3000, EYELA, Japan).

The incident solar radiation was continuously monitored by an Eldonet broadband filter radiometer (Eldonet XP, Real Time Computer, Möhrendorf, Germany) which was placed near the water bath. The fluctuating solar radiation in the present study was mainly controlled by diel variability, but additionally influenced by cloud and rain. The photoperiod during the outdoor incubation was 14:10 light:dark. We diluted the cultures and collected samples at 4:30 pm to imprint the influences of light or solar radiation during the light period. The mean daytime PAR (MDR) was taken as the averaged values over one dilution cycle (between the two sequential dilutions).

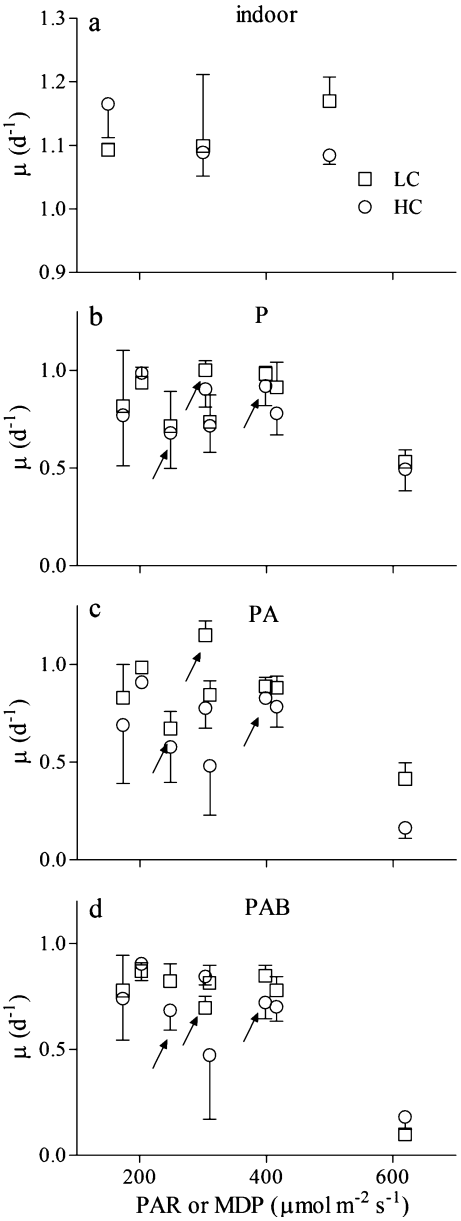

Figure 2. Growth rates of *E. huxleyi* at indoor constant (a) and outdoor (b–d) fluctuating light regimes. The mean daytime PAR (MDR) was the average value of one dilution cycle. LC represents cells grown at ambient CO_2 concentration (390 μatm), HC those grown at high CO_2 concentration (1000 μatm). Panels b, c and d are the cells exposed to P (PAR), PA (PAR + UVA), PAB (PAR + UVA + B), respectively. The black arrows indicate the growth rates at outdoor, and POC and PIC were sampled at the end of the corresponding dilution cycle (Fig. 1). Data are the means ± SD (six replicate cultures at indoor, three replicate cultures at outdoor).

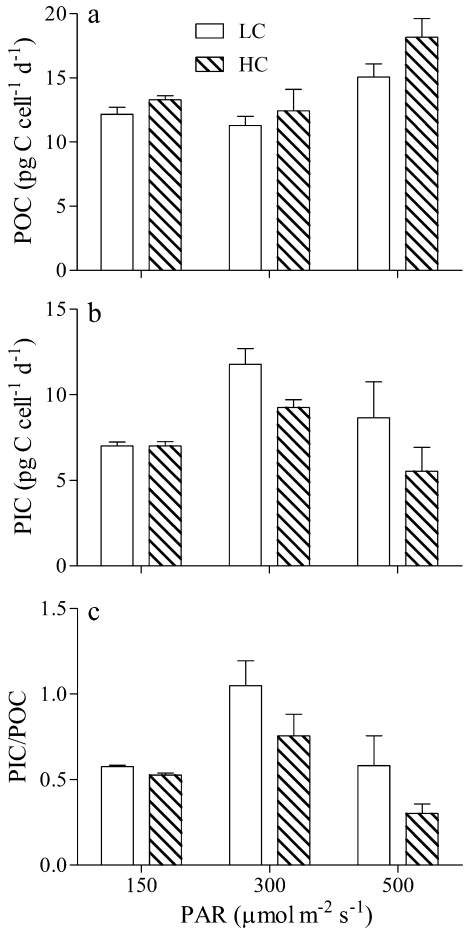

Figure 3. Particulate organic carbon (a) and PIC (b) production rates and PIC/POC ratios (c) of the *E. huxleyi* cells that grew under the indoor light regimes at ambient (390 μatm, LC) and elevated (1000 μatm, HC) CO_2 concentrations. Data are the means ± SD (three of the six replicate cultures were used for POC and PIC analysis).

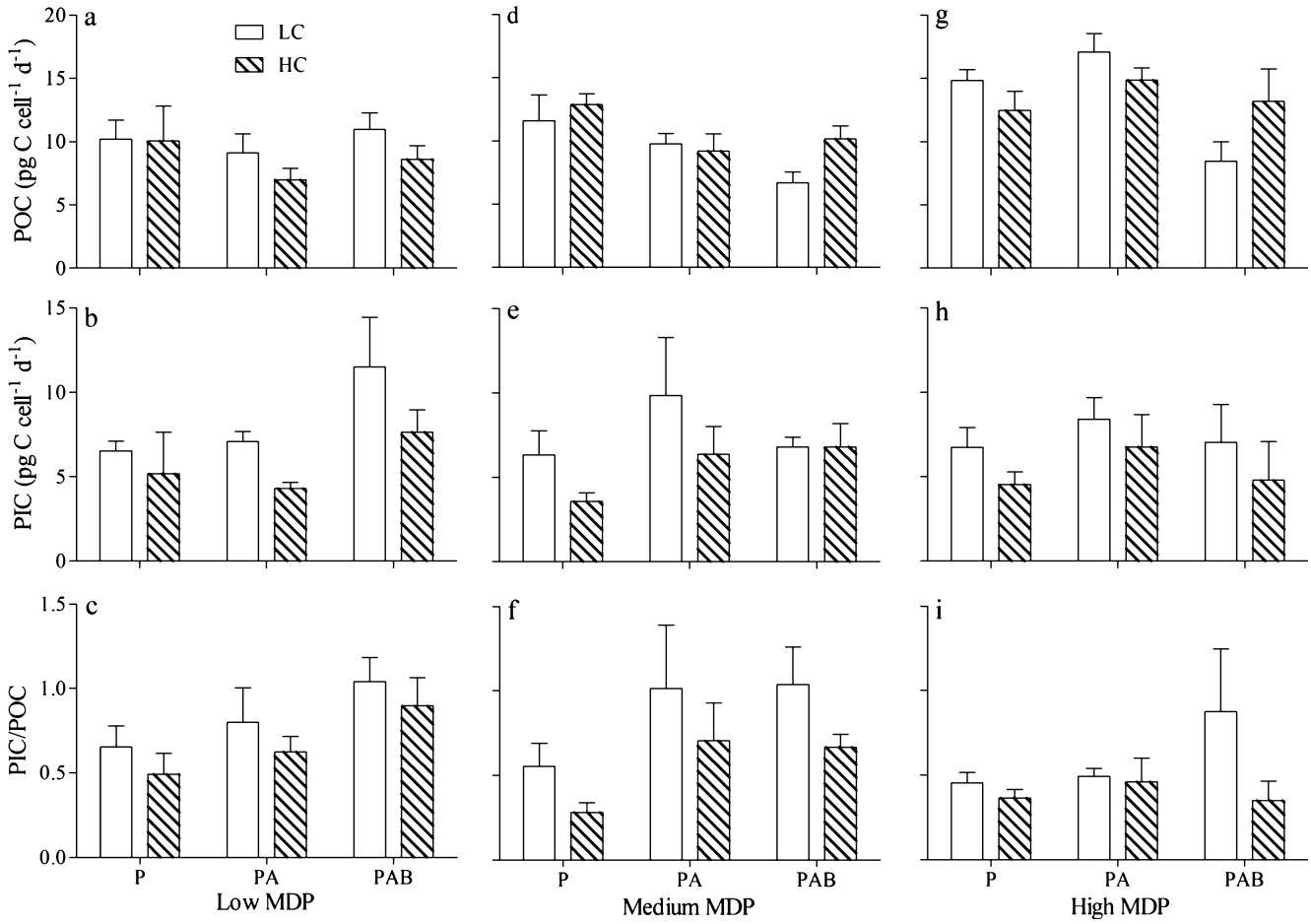

Figure 4. Particulate organic carbon (a, d, g) and PIC (b, e, h) production rates and PIC/POC ratios (c, f, i) of the *E. huxleyi* cells that grew under solar radiation at ambient (390 μatm, LC) and elevated (1000 μatm, HC) CO_2 concentrations. Data are the means ± SD (triplicate cultures). P, PA and PAB represent exposure to PAR alone, PAR + UVA and PAR + UVA + B, respectively. The low, medium and high MDP were 248 μmol m^{-2} s^{-1} (44th day), 303 μmol m^{-2} s^{-1} (41th day) and 398 μmol m^{-2} s^{-1} (54th day), respectively.

Cell concentrations were measured using a Coulter counter (Z2, Beckman Instruments, Florida, US) and specific growth rate was calculated as $\mu = (\ln N_t - \ln N_0)/t$, where N_0 and N_t are the cell concentrations right after the dilution and before the next dilution, respectively. Two subsamples from each culture were filtered on preburned GF/F filters (500°C, 3 h). One filter was rinsed with the culture medium and the other was rinsed and subsequently fumed with 38% HCl for 12 h to remove all inorganic carbon. The difference in the carbon values of the two filters is the particulate inorganic carbon (PIC) content. The production rates of PIC and particulate inorganic carbon (POC) were calculated as in the following formulae: PIC production = (PIC/cell) × μ, POC production = (POC/cell) × μ. The POC and PIC samples were taken at the 41th, 44th and 54th day with MDR of 303 μmol m^{-2} s^{-1}, 248 μmol m^{-2} s^{-1}, and 398 μmol m^{-2} s^{-1} respectively.

Diurnal changes of effective quantum yield (F_v'/F_m') were determined with a fluorescence induction and relaxation device (FIRe, Satlantic, Halifax, Canada). Firstly the actinic light level was adjusted close to the real incident PAR level, and then 4 mL cultures were used immediately to measure the fluorescence parameters according to the FIRe manual. Non-photochemical quenching (NPQ) was calculated as follows: NPQ = (F_m–F_m')/F_m', where F_m represents the maximum fluorescence yield of the cells (10 min dark treatment in the early morning, 7:00 am) and F_m' represents the maximum fluorescence yield of the cells (35).

Samples to be examined with scanning electron microscope (SEM) were gently filtered on polycarbonate filters (Whatman, pore size 1 μm) and dried at room temperature. These filters were sputter-coated with gold/palladium alloy and then examined with a Philips XL30 scanning electron microscope (Eindhoven, the Netherlands). A scale bar on each SEM figure was used to calibrate the magnification. At least 100 coccoliths and 100 coccosphere were examined per treatment. The coccoliths were identified into four categories of morphology: normal, incomplete, malformed, incomplete and malformed (36). The SEM samples of the 44th day (MDP of 303 μmol m^{-2} s^{-1}) were lost.

All statistical analyses were performed with the software R 3.10 (http://cran.r-project.org) in conjunction with functions of the Wilcox' Robust Statistics package (37). Interactive effects between factors were investigated with robust two-way and three-way analyses by procedure t2way and t3way functions, followed with multiple-comparisons by applying con2way and con3way functions. The differences between the two independent groups were analyzed by Yuen's trimmed mean test (37). These methods use 20% trimmed means as a measure of location to establish significance and were chosen over the classic *t*-test and ANOVA, because they do not have the standard assumptions of normality or homoscedasticity and generally had higher power (37). Wilcoxon's rank tests (nonparametric test) were used to analyze effects of different treatments on growth rates of cultures under solar radiation. The significance level for all of the tests was set at $P = 0.05$.

RESULTS

Carbonate system

Regardless of CO_2 concentrations, the carbonate parameter values did not exhibit significant differences among the three radiation treatments P (PAR), PA (PAR + UVA) and PAB

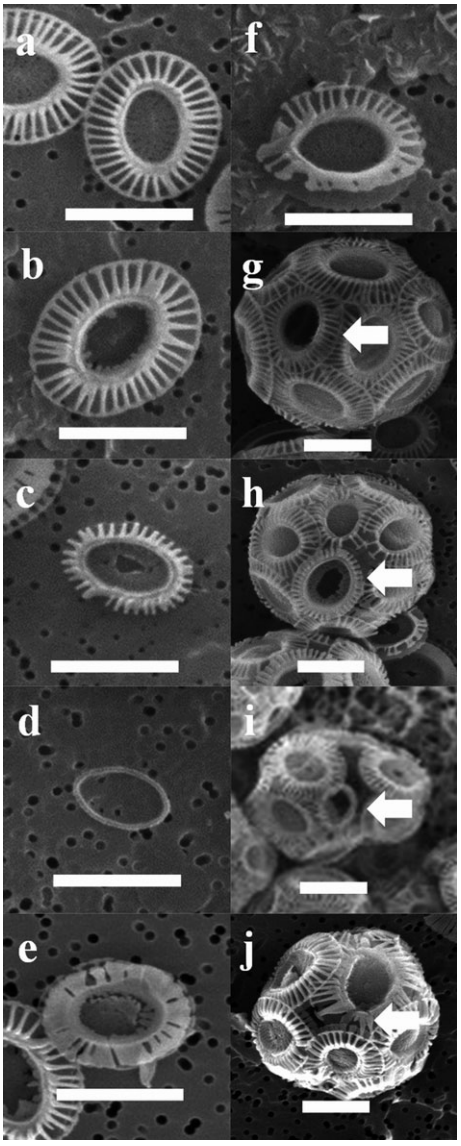

Figure 5. Different shapes of coccoliths of *E. huxleyi*: (a) nomal; (b-d) incomplete; (e) malformed; (f) incomplete and malformed (I & M). White arrows showed incomplete coccoliths (g–i) and I&M coccolith (j). All of the white bars are 2 μm.

(PAR + UVA + B) ($P > 0.05$, Table 1). The calculated pCO_2 levels in the cultures ranged between 398–402 and 978–991 μatm, under ambient (LC) and elevated (HC) CO_2 concentrations, respectively. The elevated CO_2 level decreased pH by about 0.34 unit ($P < 0.001$, Table 1), increased DIC and HCO_3^- by 7% ($P = 0.001$) and 12% ($P = 0.001$), respectively, with CO_3^{2-} concentration decreased by 48% ($P = 0.001$).

Growth rate

Under indoor constant (nonfluctuating) light regimes, the HC treatment enhanced the growth rate by 7% at 150 μmol m^{-2} s^{-1} ($P = 0.036$, Fig. 2a), while no significant influence was found at 300 μmol m^{-2} s^{-1} ($P = 0.886$) and the growth rate was reduced by 6% at 500 μmol m^{-2} s^{-1} ($P = 0.006$), compared to the LC treatment. When the cells were transferred from 500 μmol m^{-2} s^{-1} PAR regime to outdoor fluctuating solar radiation, high CO_2 significantly decreased growth rates under the PA treatment ($P = 0.008$, Fig. 2a), but no significant effects in the P ($P = 0.078$, Fig. 2b) and PAB ($P = 0.461$, Fig. 2c) treatments were observed. While there were no significant differences between the PA and PAB treatments under both CO_2 concentrations ($P > 0.05$, Fig. 2c,d), UVA induced a reduction of about 17% in the average growth rates in the HC-grown cells ($P = 0.016$, Fig. 2b,c). However, in the LC-grown cells, neither UVA ($P = 0.109$) nor UVB ($P = 0.945$) resulted in a decrease of the growth rates.

For most of the cases (15 out of 16) under P and PA treatments, the growth rates were lower under HC than under LC conditions. However, when exposed to PAB (in the presence of UVB), only five out of eight cases showed lower growth rates in HC compared to LC cultures. Moreover, for growth at the highest mean daytime PAR (MDP, 620 μmol m^{-2} s^{-1}), UVA did not affect the growth of LC-grown cells ($P = 0.065$) relative to the P treatment, but UVB decreased the growth compared with both P and PA treatments ($P < 0.001$); UVA exhibited strong negative effects on growth rates of HC-grown cells compared with P treatment ($P = 0.002$), but UVB did not further decrease the growth ($P = 0.701$).

POC and PIC

Under the indoor conditions, the HC treatment increased the POC production rate ($P = 0.007$, Fig. 3) and decreased the PIC production rate ($P = 0.009$) compared with the LC treatment, and led to a lowered PIC/POC ratio ($P = 0.003$). When compared at each light level, increased POC production rate was only significant at PAR of 500 μmol m^{-2} s^{-1} ($P = 0.048$), and decreased PIC production rate was only significant at 300 μmol m^{-2} s^{-1} ($P = 0.024$), with PIC/POC ratio being only significantly reduced by HC treatment under 150 μmol m^{-2} s^{-1} ($P = 0.005$). Regardless of the CO_2 concentrations, the maximum POC production rate appeared at a PAR level of 500 μmol m^{-2} s^{-1} ($P < 0.01$, Fig. 3a) and the maximal values of PIC production rate and PIC/POC ratio were found at 300 μmol m^{-2} s^{-1} ($P < 0.01$, Fig. 3b,c).

When the cells were transferred to the incident fluctuating solar radiation with PAR alone (P treatment), no significant effects were found on the POC production rate between HC and LC cultures ($P = 0.637$, Fig. 4a,d,g). The PIC production rates ($P = 0.011$) and PIC/POC ratio ($P = 0.004$) significantly decreased in the HC compared to the LC-grown cells. However, among the three mean daytime PAR (MDP) levels, the HC treatment only decreased the PIC production rate ($P = 0.067$, Fig. 4e) and PIC/POC ratio ($P = 0.057$, Fig. 4f) at the medium MDP on a marginally significant level.

The effects of UVR on the POC production rates appeared to depend on the MDP levels. At the low MDP level (Fig. 4a–c), the presence of UVA or UVB did not result in a significant difference in the POC production ($P > 0.05$, Fig. 4a). However, at the medium MDP level (Fig. 4d,e,f), the presence of UVA significantly reduced the POC production rate ($P = 0.018$, Fig. 4d), while UVB did not bring out a significant difference ($P = 0.65$). At the high MDP level (Fig. 4g–i), UVA significantly increased the POC production rates ($P = 0.015$, Fig. 4g), while the presence of UVB led to a significant lower POC production ($P = 0.003$). In terms of PIC production that was increased by

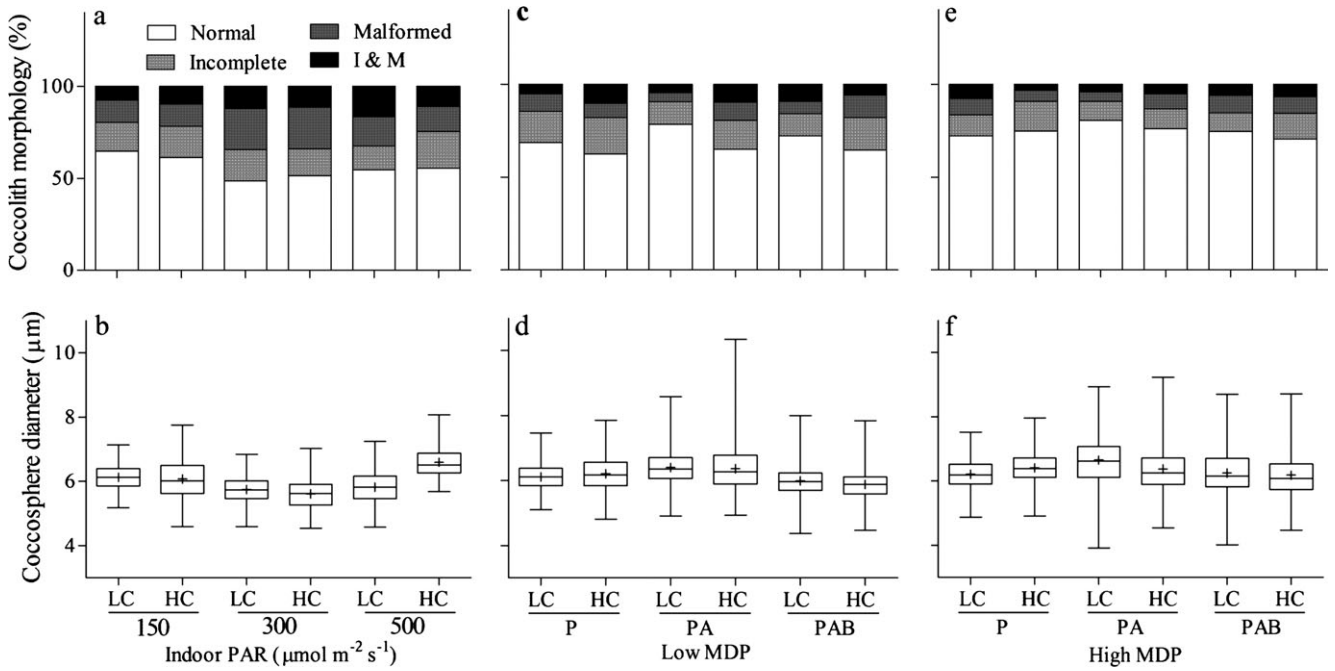

Figure 6. Panel a (under indoor constant PAR), c (under outdoor low MDP) and e (under outdoor high MDP) showed the percentages of differently shaped coccoliths. The corresponding coccosphere diameters (each treatment measured at least 100 coccosphere) were presented in panel b, d and f. P, PA and PAB represent exposed to PAR alone, PAR + UVA and PAR + UVA + B, respectively. The central marker "+" denotes the mean, the standard deviation given by the box boundaries and the whiskers represent the minimum and maximum values.

the presence of UVB, leading to a higher PIC/POC ratio ($P < 0.05$, Fig. 4b,c) relative to P and PA treatments at low MDP levels. Exposure to UVA increased the PIC production rate and PIC/POC ratio at medium MDP ($P < 0.05$, Fig. 4e,f), while UVB did not show significant effects ($P > 0.05$, Fig. 4e,f). However, at the highest MDP, the PIC production rate and PIC/POC ratio did not exhibit any significant differences among the three radiation treatments ($P > 0.05$, Fig. 4h,i). Regardless of the MDP levels or UVR, both the PIC production rate and the PIC/POC ratio significantly decreased in HC-grown cells compared to the LC treatment ($P < 0.05$, Fig. 4), but POC production rates were not altered by the OA treatment ($P > 0.05$).

Coccolith morphology and coccosphere diameter

There were four categories of coccolith morphology: normal (Fig. 5a), incomplete (Fig. 5b, unclosed central area; Fig. 5c, unclosed central area and lack of periphery; Fig. 5d, with only a coccolith ring), malformed (Fig. 5e, malformed proximal shield elements), incomplete and malformed (Fig. 5f, lack part of distal shield elements and part of distal shield elements fused). These abnormal coccoliths could still assemble into the coccosphere although their size and shapes differed among the different CO_2 and radiation treatments (Figs. 5g–j and 6).

Under the indoor constant light levels, the normal coccolith percentages for low and high CO_2 treatments were in range of 48–65% and 51–61%, respectively. In contrast, the values of normal coccolith percentage under outdoor fluctuating light conditions were higher. The normal coccolith percentages of LC and HC-grown cells ranged from 68–78% and 62–65% at the low MDP, and 72–80% and 70–76% at the high MDP, respectively.

The distribution of coccosphere size showed large variability; even within a single treatment, the maximum diameter could be up to 2 times the minimum (Fig. 6). Enhanced CO_2 did not show consistent effects on coccosphere diameter in this study. The coccosphere diameter was not significantly altered by HC treatment under the low constant PAR of 150 μmol m^{-2} s^{-1} relative to LC ($P = 0.384$, Fig. 6b), but was marginally decreased by 3% at 300 μmol m^{-2} s^{-1} ($P = 0.006$) and increased by 13% at 500 μmol m^{-2} s^{-1} ($P < 0.001$). After transfer to outdoor conditions, positive effects of high-CO_2 on coccosphere diameters were only found in the P treatment ($P < 0.05$, Fig. 6d,f). The presence of UVA increased the coccosphere diameter (but by less than 8%) in comparisons with that of PAR alone or PAR+-UVR treatments ($P < 0.001$, Fig. 6d,f).

Fluorescence parameters

Under exposures to solar radiation, the effective quantum yield, F_v'/F_m', decreased as PAR increased during the morning period, and increased with decreased PAR in the afternoon (Fig. 7). Under P or PA treatment, F_v'/F_m' did not show significant differences in the HC compared to the LC-grown cells. However, in the presence of UVB, the HC-grown cells decreased their yield tremendously during the noon period when the incident PAR levels were highest (in the range of 550–630 μmol m^{-2} s^{-1}) ($P < 0.05$, Fig. 7d). At 13:00, NPQ of the HC-grown cells was not significantly different from that of the LC-grown ones under P and PA treatments ($P > 0.05$), but the HC-grown cells significantly ($P = 0.042$) increased NPQ by 35% under exposure to PAB (with UVB) (Fig. 8). Both UVA and UVB significantly increased the NPQ of both CO_2 treatments ($P < 0.01$).

DISCUSSION

The physiological performance of photoautotrophic organisms is primarily governed by solar energy (24), however, most of these organisms are exposed to solar UV radiation in their ecological niches. In this study, we found both PAR and UVR interacted with OA (seawater pH decline/pCO_2 rise) to influence the physiological performance of the coccolithophorid *Emiliania huxleyi* CS-369. When grown under indoor constant levels (150–500 μmol m^{-2} s^{-1}) of PAR, the OA treatment increased the POC production rates and decreased the PIC production rates and PIC/POC ratios (Fig. 3). This result is consistent with a summary based on 15 studies with similar indoor PAR levels (5). Nevertheless, the effects of OA on *E. huxleyi* calcification are still under debate (3,11–13). To predict the consequences in natural marine environments, the ecological effects of OA should be investigated under different experimental set-ups to reflect multiple biotic and abiotic factors (5,6,38,39).

During the indoor growth experiments, the HC treatment with a CO_2 concentration of 1000 μatm increased the growth rate of *E. huxleyi* CS-369 at constant PAR of 150 μmol m^{-2} s^{-1} compared with those under ambient CO_2 conditions (Fig. 2a). Such a growth enhancement could be attributed to the photosynthesis-limiting light availability (40). Thus, stimulation of growth was offset by increased light levels, so that a neutral effect was observed at 300 μmol m^{-2} s^{-1} and growth inhibition by OA was observed at 500 μmol m^{-2} s^{-1}. Such an inhibitory effect of OA has been suggested to be caused by enhanced light stress (38). However, different species or strains of coccolithophores may show differential responses to OA. In contrast, the growth rate of *E. huxleyi* CCMP371 was not influenced by elevated CO_2 concentrations at a PAR level of 50 μmol m^{-2} s^{-1}, but was enhanced at 400 μmol m^{-2} s^{-1} (41). In addition, regardless of PAR levels (15–300 μmol m^{-2} s^{-1}), changes of CO_2 levels did not influence the growth of *E. huxleyi* RCC1216 (42) and PML92/11 (43). These discrepancies could be attributed to strain-specific physiological performance or to different experimental set-ups including temperature, actual CO_2 levels/ranges, light levels and nutrients availability (5,6).

During the outdoor incubation under sunlight, the levels of mean daytime PAR (MDP) ranged from 170–620 μmol m^{-2} s^{-1}, being equivalent to the indoor PAR ranges (150–500 μmol m^{-2} s^{-1}). In comparison, the average growth rates (~1.1–1.2 d^{-1}, Fig. 2 a) of *E. huxleyi* CS-369 under indoor constant PAR were higher than those under fluctuating solar PAR (~0.5–1.0 day^{-1}, Fig. 2b). Moreover, stimulative effects of HC on POC production at constant PAR levels disappeared after cultures were transferred to fluctuating sunlight (Figs. 3 and 4). In view of the highest PAR levels during the noon period, the outdoor PAR level could be over 2–3 times that of MDP or indoor ones. Obviously, the *E. huxleyi* cells suffered from more light stress when exposed under sunlight, which led to decreased F_v'/F_m' during the noon (Fig. 7). Natural light fluctuation could thus influence the growth, carbon fixation and photoprotection of phytoplankton (18,19,44). Generally, phytoplankton species increase their energy costs for maintenance and repair of photosystems to cope with fluctuating or stressful light (19). Therefore, the energy allocation of *E. huxleyi* was disturbed, leading to lowered growth rates (Fig. 2).

When the cells were exposed to solar radiation with UVR (Fig. 2), the data showed high variability. The strongest effects

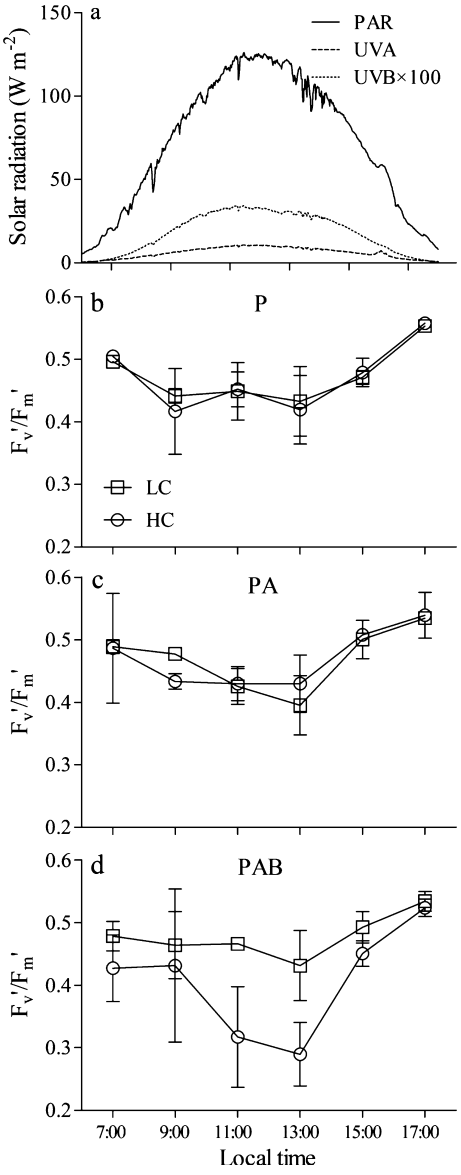

Figure 7. The diurnal change of solar radiation at day 39th (a, 2011 July 4) with MDP of 358 μmol m^{-2} s^{-1} and effective photochemical efficiency (F_v'/F_m') under P (b), PA (c) and PAB (d) treatments. Data are the means ± SD of three replicate cultures.

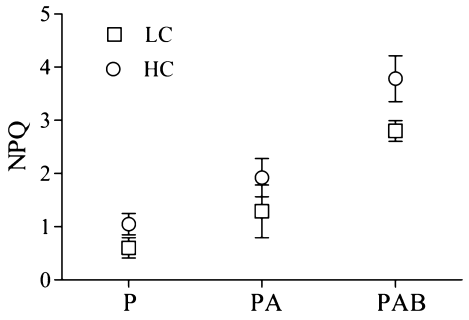

Figure 8. The interactive effects of CO_2 and UVR on NPQ of *E. huxleyi* cells. Data are the means ± SD of 3 replicate cultures.

of UVR on growth rates were found at the highest MDP, which was correlated with CO_2 concentrations. The inhibitory effects of UVA on growth were only observed in the HC-grown cells (Fig. 2). Although moderate levels of UVA can stimulate photosynthetic carbon fixation (45), in this study, our results imply that UVA could play an irrevocable role in driving the succession of phytoplankton community in future high CO_2 oceans, since it could penetrate to 118 m (1% of surface values at 340 nm) in open oceans (17). Nevertheless, little has been documented on the physiological mechanisms behind the interaction of CO_2 and UVR, considering that the primary metabolic targets of these factors are different (20).

Solar UVB irradiances often harm primary producers (21). Growth rates of *E. huxleyi* (isolated by E. Paasche, Oslo Fjord, Norway) were inhibited by 4 days exposure to UVB (46). On the other hand, OA could remediate UVB-related photochemical inhibition in the coccolithophore *Gephyrocapsa oceanica* (34). In the present work, we found that moderate levels of UVB and/or UVA marginally stimulated PIC production (Fig. 4). Enhanced calcification of the same strain of *E. huxleyi* showed less photoinhibition caused by UVR (47), reflecting a photoprotective role played by the coccolith (22,30). In addition, UVB could induce expression of defense genes of phytoplankton, activating antioxidant systems and photorepair processes (48). Calcification may serve as a defense strategy under UVR exposure since UVB photoreceptors could trigger photoprotective processes (28,49). Therefore, UVB could act as antagonistic factor to modulate the effects of OA on PIC production rate or PIC/POC ratios (Figs. 3 and 4).

Coccolithophore species, such as *E. huxleyi*, *Gephyrocapsa oceanica* and *Coccolithus pelagicus* produced more malformed coccoliths when grown at high CO_2/low pH conditions (7,8,29), though there are some other studies which reached different conclusions (13,40,50). These coccolith morphological changes may reflect strain-specific responses to variation of seawater carbonate chemistry (36). In the present study, a large difference in the percentage of normal coccoliths of *E. huxleyi* was found between indoor constant PAR and outdoor fluctuating solar radiation (Fig. 6). However, we still do not know the mechanisms of how these factors influence the morphology of coccoliths. Some basic scientific questions regarding the molecular mechanisms of the calcification process of coccolithophores remain to be discovered (25,51), which will enhance our understanding of their physiological performances under multiple ocean changes.

In view of the morphological changes in coccoliths of *E. huxleyi*, though coccosphere sizes displayed a wide range (Fig. 6), coccosphere diameters increased in the presence of UVA, but did not change to a significant extent with OA treatment. Relatively, the variation in size distribution exceeded the changes of coccosphere diameter caused by UVR and/or OA treatments. However, a recent study reported that 1340 ppmv CO_2 increased the coccosphere diameter (measured by Coulter Counter) up to 2 times relative to current CO_2 concentration (13). The discrepancies between studies may be due to the use of different strains and/or different experimental set-ups. The inner cytoplasm and outer coccolith layer of the coccosphere depend on production of organic compounds and calcification, respectively. The fact that a large proportion of coccoliths are detached from the coccosphere (52), which means that the coccosphere size could not simply correlate with POC and/or PIC contents. Changes in light levels, UVR and seawater carbonate chemistry interact to alter coccosphere diameter by influencing key physiological processes, such as photosynthesis, respiration and calcification (5,6,21).

In conclusion, both PAR and UVR could alter the effects of OA on the growth rate and POC production of *E. huxleyi* CS-369. However, increased acidity of seawater under elevated CO_2 assuredly reduced the PIC production and PIC/POC ratios regardless of light levels or presence of UVR, though UVR appeared to stimulate PIC production. This suggests that progressive OA could affect the ballast effects of $CaCO_3$ on POC transport to deep oceans (53,54), though knowledge is still limited in terms of diversified coccolithophore species and strains, that may perform differently under multiple ocean changes.

Acknowledgements—We thank Tao Xing for his experimental assistance, Ru Xue from the SEM laboratory at College of Chemistry and Chemical Engineering (Xiamen University) for technical support in regard to scanning electron microscopy. This study was supported by the National Natural Science Foundation (41430967; 41120164007), Joint project of NSFC and Shandong province (Grant U1406403), the Strategic Priority Research Program of CAS (Grant XDA11020302), the Program for Changjiang Scholars and Innovative Research Team (IRT-13R51), SOA (GASI-03-01-02-04), and the China-Japan collaboration Project from MOST (S2012GR0290).

REFERENCES

1. Milliman, J. D. (1993) Production and accumulation of calcium carbonate in the ocean: budget of a nonsteady state. *Global Biogeochem. Cycles* **7**, 927–957.
2. Rost, B. and U. Riebesell (2004) Coccolithophores and the biological pump: responses to environmental changes. In *Coccolithophores: from molecular processes to global impact* (Edited by H. R. Thierstein and J. R. Young), pp. 76–99. Springer, Berlin, Germany.
3. Beaufort, L., I. Probert, T. de Garidel-Thoron, E. M. Bendif, D. Ruiz-Pino, N. Metzl, C. Goyet, N. Buchet, P. Coupel, M. Grelaud, B. Rost, R. E. M. Rickaby and C. de Vargas (2011) Sensitivity of coccolithophores to carbonate chemistry and ocean acidification. *Nature* **476**, 80–83.
4. Hofmann, G. E., J. P. Barry, P. J. Edmunds, R. D. Gates, D. A. Hutchins, T. Klinger and M. A. Sewell (2010) The effect of ocean acidification on calcifying organisms in marine ecosystems: an organism to ecosystem perspective. *Annu. Rev. Ecol. Evol. Syst.* **41**, 127–147.
5. Riebesell, U. and P. D. Tortell (2011) Effects of ocean acidification on pelagic organisms and ecosystems. In *Ocean acidification* (Edited by J. P. Gattuso and L. Hansson), pp. 99–121. Oxyford University Press, Oxyford.
6. Gao, K., E. W. Helbling, D. P. Häder and D. A. Hutchins (2012) Responses of marine primary producers to interactions between ocean acidification, solar radiation, and warming. *Mar. Ecol. Prog. Ser.* **470**, 167–189.
7. Riebesell, U., I. Zondervan, B. Rost, P. D. Tortell, R. E. Zeebe and F. M. M. Morel (2000) Reduced calcification of marine plankton in response to increased atmospheric CO_2. *Nature* **407**, 364–367.
8. Rickaby, R. E. M., J. Henderiks and J. N. Young (2010) Perturbing phytoplankton: response and isotopic fractionation with changing carbonate chemistry in two coccolithophore species. *Clim. Past* **6**, 771–785.
9. Jin, P., K. Gao and J. Beardall (2013) Evolutionary responses of a coccolithophorid *Gephyrocapsa oceanica* to ocean acidification. *Evolution* **67**, 1869–1878.
10. Sett, S., L. T. Bach, K. G. Schulz, S. Koch-Klavsen, M. Lebrato and U. Riebesell (2014) Temperature modulates coccolithophorid sensitivity of growth, photosynthesis and calcification to increasing seawater pCO_2. *PLoS One* **9**, e88308.

11. Iglesias-Rodriguez, M. D., P. R. Halloran, R. E. M. Rickaby, I. R. Hall, E. Colmenero-Hidalgo, J. R. Gittins, D. R. H. Green, T. Tyrrell, S. J. Gibbs, P. Von Dassow, E. Rehm, E. V. Armbrust and K. P. Boessenkool (2008) Phytoplankton calcification in a high-CO_2 world. *Science* **320**, 336–340.
12. Shi, D., Y. Xu and F. M. M. Morel (2009) Effects of the pH/pCO_2 control method on medium chemistry and phytoplankton growth. *Biogeosciences* **6**, 1199–1207.
13. Jones, B. M., M. D. Iglesias-Rodriguez, P. J. Skipp, R. J. Edwards, M. J. Greaves, J. R. Young, H. Elderfield and C. D. O'Connor (2013) Responses of the *Emiliania huxleyi* proteome to ocean acidification. *PLoS One* **8**, e61868.
14. IPCC (2001) *IPCC Climate Change 2001: The Scientific Basis*. United Kingdom, New York, USA, Cambridge University Press, Cambridge.
15. Doney, S. C. (2006) Plankton in a warmer world. *Nature* **444**, 695–696.
16. Capotondi, A., M. A. Alexander, N. A. Bond, E. N. Curchitser and J. D. Scott (2012) Enhanced upper ocean stratification with climate change in the CMIP3 models. *J. Geophys. Res.* **117**, C04031.
17. Tedetti, M., R. Sempéré, A. Vasilkov, B. Charrière, D. Nérini, W. L. Miller, K. Kawamura and P. Raimbault (2007) High penetration of ultraviolet radiation in the south east Pacific waters. *Geophys. Res. Lett.* **34**, L12610.
18. Wagner, H., T. Jakob and C. Wilhelm (2006) Balancing the energy flow from captured light to biomass under fluctuating light conditions. *New Phytol.* **169**, 95–108.
19. Dimier, C., C. Brunet, R. Geider and J. Raven (2009) Growth and photoregulation dynamics of the picoeukaryote *Pelagomonas calceolata* in fluctuating light. *Limnol. Oceanogr.* **54**, 823–836.
20. Beardall, J., C. Sobrino and S. Stojkovic (2009) Interactions between the impacts of ultraviolet radiation, elevated CO_2, and nutrient limitation on marine primary producers. *Photochem. Photobiol. Sci.* **8**, 1257–1265.
21. Häder, D. P., E. W. Helbling, C. E. Williamson and R. C. Worrest (2011) Effects of UV radiation on aquatic ecosystems and interactions with climate change. *Photochem. Photobiol. Sci.* **10**, 242–260.
22. Gao, K., Z. Ruan, V. E. Villafañe, J. P. Gattuso and E. W. Helbling (2009) Ocean acidification exacerbates the effect of UV radiation on the calcifying phytoplankter *Emiliania huxleyi*. *Limnol. Oceanogr.* **54**, 1855–1862.
23. Guan, W. and K. Gao (2010) Impacts of UV radiation on photosynthesis and growth of the coccolithophore *Emiliania huxleyi* (Haptophyceae). *Environ. Exp. Bot.* **67**, 502–508.
24. Falkowski, P. G. and J. A. Raven (2007) *Aquatic photosynthesis*. Princeton University Press, Princeton, New Jersey.
25. Mackinder, L., G. Wheeler, D. Schroeder, U. Riebesell and C. Brownlee (2010) Molecular mechanisms underlying calcification in coccolithophores. *Geomicrobiol. J.* **27**, 585–595.
26. Brownlee, C. and A. Taylor (2004) Calcification in coccolithophores: a cellular perspective. In *Coccolithophores: from molecular processes to global impact* (Edited by H. R. Thierstein and J. R. Young), pp. 31–49. Springer, Berlin, Germany.
27. Xu, K., K. Gao, V. E. Villafañe and E. W. Helbling (2011) Photosynthetic responses of *Emiliania huxleyi* to UV radiation and elevated temperature: roles of calcified coccoliths. *Biogeosciences* **8**, 1441–1452.
28. Barcelos e Ramos, J., K. Schulz, S. Febiri and U. Riebesell (2012) Photoacclimation to abrupt changes in light intensity by *Phaeodactylum tricornutum* and *Emiliania huxleyi*: the role of calcification. *Mar. Ecol. Prog. Ser.* **452**, 11–26.
29. Bach, L. T., C. Bauke, K. J. S. Meier, U. Riebesell and K. G. Schulz (2012) Influence of changing carbonate chemistry on morphology and weight of coccoliths formed by *Emiliania huxleyi*. *Biogeosciences* **9**, 3449–3463.
30. Xu, K. and K. Gao (2012) Reduced calcification decreases photoprotective capability in the coccolithophorid *Emiliania huxleyi*. *Plant Cell Physiol.* **53**, 1267–1274.
31. Price, N. M., G. I. Harrison, J. G. Hering, R. J. Hudson, P. M. V. Nirel, B. Palenik and F. M. M. Morel (1988/89) Preparation and chemistry of the artificial algal culture medium Aquil. *Biol. Oceanogr.* **6**, 443–461.
32. Dickson, A., J. Afghan and G. Anderson (2003) Reference materials for oceanic CO_2 analysis: a method for the certification of total alkalinity. *Mar. Chem.* **80**, 185–197.
33. Lewis, E. and D. W. R. Wallace (1998) *Program developed for CO_2 system calculations*. ORNL/CDIAC-105. Carbon Dioxide Information Analysis Center, Oak Ridge National Laboratory, US Department of Energy, Oak Ridge, Tennessee.
34. Zheng, Y. and K. Gao (2009) Impacts of solar UV radiation on the photosynthesis, growth, and UV-absorbing compounds in *Gracilaria lemaneiformis* (Rhodophyta) grown at different nitrate concentrations. *J. Phycol.* **45**, 314–323.
35. Bilger, W. and O. Björkman (1990) Role of the xanthophyll cycle in photoprotection elucidated by measurements of light-induced absorbance changes, fluorescence and photosynthesis in leaves of Hedera canariensis. *Photosynth. Res.* **25**, 173–185.
36. Langer, G., I. Probert, G. Nehrke and P. Ziveri (2011) The morphological response of *Emiliania huxleyi* to seawater carbonate chemistry changes: an inter-strain comparison. *J. Nannoplankton Res.* **32**, 29–34.
37. Wilcox, R. R. (2012) *Introduction to robust estimation and hypothesis testing*. Academic Press, Boston, MA.
38. Gao, K. and D. A. Campbell (2014) Photophysiological responses of marine diatoms to elevated CO_2 and decreased pH: a review. *Funct. Plant Biol.* **41**, 449.
39. Beardall, J., S. Stojkovic and K. Gao (2014) Interactive effects of nutrient supply and other environmental factors on the sensitivity of marine primary producers to ultraviolet radiation: implications for the impacts of global change. *Aquat. Biol.* doi:10.3354/ab00582.
40. Zondervan, I. (2007) The effects of light, macronutrients, trace metals and CO_2 on the production of calcium carbonate and organic carbon in coccolithophores—a review. *Deep-Sea Res. II* **54**, 521–537.
41. Feng, Y., M. E. Warner, Y. Zhang, J. Sun, F.-X. Fu, J. M. Rose and D. A. Hutchins (2008) Interactive effects of increased pCO_2, temperature and irradiance on the marine coccolithophore *Emiliania huxleyi* (Prymnesiophyceae). *Eur. J. Phycol.* **43**, 87–98.
42. Rokitta, S. D. and B. Rost (2012) Effects of CO_2 and their modulation by light in the life-cycle stages of the coccolithophore *Emiliania huxleyi*. *Limnol. Oceanogr.* **57**, 607–618.
43. Zondervan, I., B. Rost and U. Riebesell (2002) Effect of CO_2 concentration on the PIC/POC ratio in the coccolithophore *Emiliania huxleyi* grown under light-limiting conditions and different daylengths. *J. Exp. Mar. Biol. Ecol.* **272**, 55–70.
44. Jin, P., K. Gao, V. E. Villafañe, D. A. Campbell and W. Helbling (2013) Ocean acidification alters the photosynthetic responses of a coccolithophorid to fluctuating UV and visible radiation. *Plant Physiol.* **162**, 2084–2094.
45. Gao, K., Y. Wu, G. Li, H. Wu, V. E. Villafañe and E. W. Helbling (2007) Solar UV radiation drives CO_2 fixation in marine phytoplankton: a double-edged sword. *Plant Physiol.* **144**, 54–59.
46. Buma, A. G. J., T. van Oijen, W. van De Poll, M. J. W. Veldhuis and W. W. C. Gieskes (2000) The sensitivity of *Emiliania huxleyi* (Prymnesiophyceae) to ultraviolet-B radiation. *J. Phycol.* **36**, 296–303.
47. Guan, W. and K. Gao (2010) Enhanced calcification ameliorates the negative effects of UV radiation on photosynthesis in the calcifying phytoplankter *Emiliania huxleyi*. *Chin. Sci. Bull.* **55**, 588–593.
48. Häder, D. P., H. Kumar, R. Smith and R. Worrest (2007) Effects of solar UV radiation on aquatic ecosystems and interactions with climate change. *Photochem. Photobiol. Sci.* **6**, 267–285.
49. Wu, D., Q. Hu, Z. Yan, W. Chen, C. Yan, X. Huang, J. Zhang, P. Yang, H. Deng, J. Wang, X. Deng and Y. Shi (2012) Structural basis of ultraviolet-B perception by UVR8. *Nature* **484**, 214–219.
50. Lefebvre, S. C., I. Benner, J. H. Stillman, A. E. Parker, M. K. Drake, P. E. Rossignol, K. M. Okimura, T. Komada and E. J. Carpenter (2012) Nitrogen source and pCO_2 synergistically affect carbon allocation, growth and morphology of the coccolithophore *Emiliania huxleyi*: potential implications of ocean acidification for the carbon cycle. *Global Change Biol.* **18**, 493–503.
51. Jones, B. M., R. J. Edwards, P. J. Skipp, C. D. O'Connor and M. D. Iglesias-Rodriguez (2011) Shotgun proteomic analysis of *Emiliania huxleyi*, a marine phytoplankton species of major biogeochemical importance. *Mar. Biotechnol.* **13**, 496–504.
52. Paasche, E. (2002) A review of the coccolithophorid *Emiliania huxleyi* (Prymnesiophyceae), with particular reference to growth,

coccolith formation, and calcification-photosynthesis interactions. *Phycologia* **40**, 503–529.
53. Armstrong, R. A., C. Lee, J. I. Hedges, S. Honjo and S. G. Wakeham (2001) A new, mechanistic model for organic carbon fluxes in the ocean based on the quantitative association of POC with ballast minerals. *Deep Sea Res. Part II: Topic. Stud. Oceanog.* **49**, 219–236.
54. Klaas, C. and D. E. Archer (2002) Association of sinking organic matter with various types of mineral ballast in the deep sea: implications for the rain ratio. *Global Biogeochem. Cycles* **16**, 1116.